Published for SISSA by Springer

Received: *December 15, 2017*
Accepted: *February 25, 2018*
Published: *March 26, 2018*

Resonant production of Wh and Zh at the LHC

Antonio Dobado, Felipe J. Llanes-Estrada and Juan J. Sanz-Cillero

Departamento de Física Teórica, Universidad Complutense de Madrid, Plaza de las Ciencias 1, 28040 Madrid, Spain

E-mail: dobado@fis.ucm.es, fllanes@fis.ucm.es, jjsanzcillero@ucm.es

Abstract: We examine the production of Wh and Zh pairs at the LHC in the context of a Strongly Interacting Symmetry Breaking Sector of the Standard Model. Our description is based on a non-linear Higgs Effective Theory, including only the Standard Model particles. We focus on its scalar sector (Higgs boson h and electroweak Goldstones associated to $W_L^{\pm}$ and Z_L), which is expected to give the strongest beyond Standard Model rescattering effects. The range of the effective theory is extended with dispersion-relation based unitarization, and compared to the alternative extension with explicit axial-vector resonances. We estimate the Wh and Zh production cross-section, where an intermediate axial-vector resonance is generated for certain values of the chiral couplings. We exemplify our analysis with a benchmark axial-vector with $M_A = 3\,\text{TeV}$. Interestingly enough, these different approaches provide essentially the same prediction. Finally we discuss the sensitivity of ATLAS and CMS to such resonances.

Keywords: Chiral Lagrangians, Effective Field Theories, Higgs Physics, Technicolor and Composite Models

ArXiv ePrint: 1711.10310

https://doi.org/10.1007/JHEP03(2018)159

JHEP03(2018)159

Contents

1 Introduction **1**

2 Low-energy EFT **3**
- 2.1 Leading order Lagrangian 3
- 2.2 Next-to-leading order effective Lagrangian 5

3 The elementary subprocesses $q\overline{q'} \to W_L/Z_L + h$ at leading order **6**

4 The strongly interacting W_Lh and Z_Lh amplitudes **8**

5 The axial-vector form factor up to NLO in HEFT **13**

6 The axial form factor in the resonance region **15**
- 6.1 AFF with a resonance Lagrangian 15
- 6.2 Unitarized HEFT parametrizations of the axial form factor 16

7 Cross section from intermediate gauge boson production **18**

8 Conclusions **20**

1 Introduction

If physics beyond the Standard Model exists, the absence of new physics states in the few-hundred GeV region and the lightness of the new Higgs-like boson naturally suggest some new strongly interacting sector with an additional (pseudo) Goldstone boson beyond the three needed for the Electroweak Chiral Symmetry Breaking. This would call for enlarging the Standard Model (SM) symmetry group, leading perhaps to Composite Higgs Models.

A complete exploration of the Goldstone boson scattering in those SM extensions may provide important information on their underlying nature. This requires not only an examination of V_LV_L but also V_Lh amplitudes, with $V = W^\pm, Z$. For $M_{W,Z} \ll \sqrt{s}$, the scattering of longitudinal component V_L of the massive electroweak (EW) gauge bosons is related to EW Goldstone (ω^a) processes by the equivalence theorem (ET) [1–9]: $T(V_L^aV_L^b \to V_L^cV_L^d) \simeq T(\omega^a\omega^b \to \omega^c\omega^d)$, $T(V_L^ah \to V_L^ah) \simeq -T(\omega^ah \to \omega^ah)$. We will extract the latter amplitude within the ET regime $M_{W,Z} \ll \sqrt{s}$ and neglect the $W^\pm$ and Z masses. Furthermore, since numerically $M_{q,\ell} \ll M_{W,Z} \lesssim M_h$ $(q \neq t)$,[1] all the masses of the remaining SM particles and their Yukawa couplings will also be neglected.

[1]The top quark is not considered in this analysis and its impact in these scattering processes via loops deserves a separate dedicated analysis. Nonetheless, some estimates point out that these fermion corrections are subdominant [12, 13], as the scalar boson derivative interactions eventually win over the non-derivative Yukawa contributions.

JHEP03(2018)159

There are several approaches to describing a modified SM including a Strongly Interacting Symmetry Breaking Sector (SISBS). The existence of a large mass gap between the SM and possible new physics particles points out to effective field theories (EFT) as the most convenient and model independent framework for the study of beyond SM (BSM) scenarios. Likewise, we consider the non-linear representation of the EW Goldstones, as it provides the most general SM extension allowed by symmetry [10, 11]. Irrespective of the validity of those Composite Higgs Models (CHM), the ωh scattering can be addressed in perturbation theory within the Higgs Effective Field Theory (HEFT)[2] [10, 14, 15]. It describes the interactions of the would-be-Goldstone bosons ω^a from the spontaneous EW symmetry breaking. Following the CCWZ formalism [16, 17] the ω^a transform non-linearly under chiral transformations and parametrize the coset $\mathcal{G}/\mathcal{H}$, with the EW chiral group $\mathcal{G} = \mathrm{SU}(2)_L \times \mathrm{SU}(2)_R$ and the global custodial vector subgroup $\mathcal{H} = \mathrm{SU}(2)_{R+L=C}$. HEFT extends the Higgsless Electroweak Chiral Lagrangian (EWχL) [18–21] by the addition of one singlet scalar Higgs field h with generic couplings [14, 15]; in this theory, one is agnostic about the nature of the Higgs, which is coupled as the most general scalar boson that does not disrupt the pattern of global electroweak symmetry breaking $\mathrm{SU}(2)_L \times \mathrm{SU}(2)_R \to \mathrm{SU}(2)_{L+R=C}$. Chiral symmetry $\mathcal{G}$ is spontaneously broken down to the global custodial vector subgroup $\mathcal{H}$. The EWχL implements the $\mathcal{G}$ symmetry of the SM scalar sector (and its custodial subgroup $\mathcal{H} \subset \mathcal{G}$). In order to avoid large new physics corrections to the oblique T-parameter [22], one must assume that these are also approximate symmetries of our BSM extension. The EWχL has been successfully used in the description of EW precision observables in the past, pointing out the experimental suppression of custodial symmetry breaking and supporting the consistency of the EWχL theoretical framework in the original Higgsless EWχL approach [21, 23], including Higgs effects in the EFT [24–26] and even in BSM chiral extensions of the HEFT including the Higgs and additional heavy resonance fields [25, 27, 28].

The subgroup $\mathrm{SU}(2)_L \times \mathrm{U}(1)_Y \subset \mathcal{G}$ is then gauged, like in the SM, and this introduces the coupling to the transverse gauge bosons (and thus, to the quark constituents of the proton). We will assume that the only sources of custodial symmetry breaking are the gauging of the $\mathrm{U}(1)_Y$ group and the mass splitting between the up and down components of the doublets (irrelevant in this analysis). Hence, additional $\mathrm{SU}(2)_{R+L}$ breaking operators only appear at higher orders in the HEFT, being further suppressed. This is consistent with the phenomenology, as mentioned above, and the assumption that the BSM strongly interacting sector has the same symmetries as the SM scalar sector, custodial symmetry being broken through a weak perturbative interaction with the SM gauge bosons and fermions.

The effect of the top-bottom mass splitting, another source of custodial isospin breaking, has been recently considered in [12]. Because we are working in the TeV region, both masses are approximately zero and custodial isospin is formally a good approximation. This is because the elastic $2 \to 2$ boson amplitudes are of order s/v^2 at tree level while those involving the fermions (and at the forefront, the top) are of order $\sqrt{s}m_t/v^2$, thus suppressed respect to the other ones by $m_t/\sqrt{s} \sim 0.1$ (factor that is squared upon computing

[2]Not to be confused with a similarly named earlier theory that required the top to be much heavier than the Higgs and consisted of an expansion in inverse powers of M_t.

JHEP03(2018)159

a cross section or a resonance width). The most interesting effect [12] is to perturbatively open the $t\bar{t}$ decay channel to custodial-isospin 0 and 1 resonances. An effect over any isospin 1/2 Wh resonances would be even smaller. Nevertheless, the elastic amplitudes have a potentially numerically small factor, a^2-1 or a^2-b (the last one relevant for this work), that in certain regions of the a, b parameter space can overcome the power counting. A work is in preparation that addresses this possibility.

In preparing this article we have kept in mind some recent hints in the Vh searches in ATLAS [29], where a 3.3σ (2.2σ) local (global) significance excess has been reported at $M_{Vh}\approx 3\,\text{TeV}$. However, this excess has not been confirmed by CMS [30–32], so we do not commit to a fixed energy scale for any Vh resonances. Nonetheless, we consider it useful to show that such phenomenon can be naturally described by the HEFT in the axial-vector Vh channel with $IJ=11$ quantum numbers. Thus, as a case of study, we will consider a benchmark scenario with a resonance mass $M_A=3\,\text{TeV}$ and explore the feasibility of its search at the LHC.

The low-energy EFT is introduced in section 2. In section 3, we compute the most relevant LHC subprocess, $q\bar{q}'\to V_Lh$, for the production of axial-vector resonances in the V_Lh channel. Possible BSM effects are parametrized in an axial-vector form-factor $\mathcal{F}_A(s)$ defined therein. The strong V_Lh rescattering in the HEFT, its unitarization and the generation of an axial-vector resonance are discussed in section 4. The low-energy form-factor $\mathcal{F}_A(s)$ within the HEFT is computed in section 5 and its extension up to the resonance region is provided in section 6. For this, we consider models with alternative unitarization procedures or with explicit resonance Lagrangians, all of them leading to identical conclusions. In section 7 we perform a phenomenological analysis of the $W^\pm h$ production cross section at the LHC for the referred SISBS benchmark point, with an $M_A=3\,\text{TeV}$ resonance. Finally, some concluding remarks are provided in section 8.

2 Low-energy EFT

2.1 Leading order Lagrangian

At leading order, the Lagrangian of the scalar symmetry breaking sector (SBS), the modified SBS of the SM, is an $\text{SU}(2)_L\times\text{U}(1)_Y$ gauged $\text{SU}(2)_L\times\text{SU}(2)_R/\text{SU}(2)_C$ non-linear sigma model HEFT which includes the Higgs field h as a singlet. Including chirally interacting fermions, the lowest order (LO) SISBS Lagrangian reads [12]

$$\begin{aligned}\mathcal{L}_{\text{LO}} = &\frac{v^2}{4}F(h)Tr\left\{(D_\mu U)^\dagger D^\mu U\right\}+\frac{1}{2}\partial_\mu h\partial^\mu h\\ &-V(h)+i\overline{Q}\gamma^\mu d_\mu Q-vG(h)\left[\bar{Q}'_L U H_Q Q'_R+\text{h.c.}\right],\end{aligned}\tag{2.1}$$

where the matrix field $\text{U}(\omega)\in\text{SU}(2)$ describes the EW would-be Goldstone fields (thus, by the ET, it gives us the W_L, Z_L terms of the Lagrangian) and parametrizes the coset $\text{SU}(2)_L\times\text{SU}(2)_R/\text{SU}(2)_C$.

The matrix U is equivalently described by any unitary matrix that fulfills $U=1+i\sigma_a\omega^a/v+\mathcal{O}(\omega^2)$. In particular, in the spherical representation, the would-be Goldstone

JHEP03(2018)159

fields ω^a are parametrized in the form

$$U = \sqrt{1 - \frac{\omega^2}{v^2}} + i\frac{\bar{\omega}}{v}, \tag{2.2}$$

where $\bar{\omega} = \sigma_i \omega^i$ and $v = 0.246\,\text{TeV}$ the Higgs vacuum expectation value (vev).

The $\text{SU}(2)_L \times \text{U}(1)_Y$ covariant derivative is then given by

$$D_\mu U = \partial_\mu U - ig\frac{\sigma_i}{2} W_\mu^i U + ig' U \frac{\sigma_3}{2} B_\mu. \tag{2.3}$$

In turn, the Higgs potential and the functions $F(h)$ and $G(h)$ are taken to have an analytical expansion in powers of h around $h = 0$

$$\begin{aligned} F(h) &= 1 + \sum_{n=1}^{\infty} f_n \left(\frac{h}{v}\right)^n = 1 + 2a\frac{h}{v} + b\left(\frac{h}{v}\right)^2 + \mathcal{O}(h^3)\,, \\ G(h) &= 1 + \sum_{n=1}^{\infty} g_n \left(\frac{h}{v}\right)^n\,, \\ V(h) &= v^4 \sum_{n=2}^{\infty} V_n \left(\frac{h}{v}\right)^n\,. \end{aligned} \tag{2.4}$$

In the SM one has $a = 1$, $b = a^2$, $g_1 = 1$, $V_2 = V_3 = M_h^2/2v^2$, $V_4 = M_h^2/8v^2$ and $f_{n\geq 3} = g_{n\geq 2} = V_{n\geq 5} = 0$. Deviations from these values imply new physics. While we use an expansion controlled by $1/v$ powers, if there turns out to be a new scale f such that $1/f$ is the relevant parameter for a part of the effective theory, it can be incorporated into our analysis by rescaling the coefficients of that part of the Lagrangian, that would absorb the ratio of the two scales. These chiral countings provide the most general low-energy EFT; the linear theory built on the Standard Model has some additional correlations among low-energy constants (so it is a bit less general). The relation between the two countings has been discussed at length, see for example [10, 33].

Even though the low-energy parameters could be determined from the underlying theory if it was known, from a bottom-up approach the effective couplings are in principle independent from each other and must be extracted from experimental data. Furthermore, one naturally expects that some parameters are larger than others as specific low-energy couplings are related to resonances with specific quantum numbers in the underlying theory, in principle with different masses and couplings [34, 35]. But as a low energy theory of many models of interest (CHM, dilaton models, etc.), we take the coefficients of the Higgs self-potential to scale as powers of the Higgs mass so that they are negligible against the derivative couplings in the TeV region where resonances may be found ($s \gg M_h^2$), and thus we set $V(h) \simeq 0$ as in earlier work [36]. This approximation is consistent with our use of the Equivalence Theorem, $M_W^2 \sim M_h^2 \ll s$.

In the TeV region, we see once more that all masses (especially the masses of the light quarks, most abundant in the proton) are negligible: $s \gg M_t, M_b, \ldots$. Therefore, the Yukawa interactions in eq. (2.1) are in turn negligible, and thus we set $G(h) \simeq 0$ in this work. This means that the leading process producing a $V_L h$ pair is the chain

JHEP03(2018)159

proceeding by an intermediate transverse gauge boson, and not the direct emission of a longitudinal one from the fermions. As the scope of this work is to address $W_L h$ couplings, the possible appearance of the resonances in fermionic channels is not treated and has been presented elsewhere [12]. In principle, top contributions are numerically relevant in the low-energy region, specially near threshold. Because of this, ref. [13] performed a study of the heavy fermion loops in WZ resonant production based on [37], finding that its relative importance decreased with the energy and was highly suppressed for resonances with masses $M_R \gtrsim 2\,\text{TeV}$. Taken this into account, fermion loops are out of the scope of this first estimate of the Wh resonant production cross section for an axial-vector resonance with mass $M_A \sim 3\,\text{TeV}$, and we postpone the computation of these subtle contributions for a future work.

2.2 Next-to-leading order effective Lagrangian

One peculiarity of the HEFT is that the operators χ_k of the effective Lagrangian are organized according to their chiral dimension in the form $\chi_k \sim \mathcal{O}(p^{\hat{d}\geq 2})$. A detailed summary of this counting can be found in [10]: $\partial_\mu, g, y \sim \mathcal{O}(p)$, where g and y refer to gauge and Yukawa couplings, respectively;[3] consistently, all the SM particle masses are soft scales of the HEFT, $M_{h,W,Z,t,b,\ldots} \sim \mathcal{O}(p)$; bosonic fields and fermion bilinears scale, respectively, like $\mathcal{O}(1)$ and $\mathcal{O}(p)$. Further clarifications can be found in [33, 35, 38, 39]. One can easily check that the Lagrangian (2.1) in the previous section scales like $\mathcal{O}(p^2)$ under these rules and provides the lowest order effective theory. At next-to-leading order (NLO), $\mathcal{O}(p^4)$, the relevant ωh interaction and production will be provided by the Lagrangian [14, 15, 34, 35, 40],

$$\begin{aligned}\mathcal{L}_{\text{NLO}} = {} & d\,\frac{(\partial_\mu h \partial^\mu h)}{v^2}\,\text{Tr}\{D_\nu U^\dagger D^\mu U\} + e\,\frac{(\partial_\mu h \partial^\nu h)}{v^2}\,\text{Tr}\{D^\mu U^\dagger D_\nu U\} \\ & -i f_9\,\frac{(\partial_\mu h)}{v}\,\text{Tr}\{\hat{W}^{\mu\nu}\,D_\nu U\,U^\dagger - \hat{B}^{\mu\nu}\,U^\dagger\,D_\nu U\}\,,\end{aligned} \tag{2.5}$$

where we used for the field-strength tensors the notation from [35]:

$$\begin{aligned}\hat{W}_{\mu\nu} &= \partial_\mu \hat{W}_\nu - \partial_\nu \hat{W}_\mu - i[\hat{W}_\mu, \hat{W}_\nu]\,, & \hat{B}_{\mu\nu} &= \partial_\mu \hat{B}_\nu - \partial_\nu \hat{B}_\mu - i[\hat{B}_\mu, \hat{B}_\nu]\,, \\ \hat{W}_\mu &= -\frac{g W^a_\mu \sigma_a}{2}\,, & \hat{B}_\mu &= -\frac{g' B_\mu \sigma_3}{2}\,. \end{aligned} \tag{2.6}$$

As earlier in eq. (2.4) all the "coefficients" in front of the Lagrangian operators are promoted to actual functions of the Higgs field with an analytical expansion in powers of h around $h = 0$. For example, f_9 is really the first term in an expansion $\mathcal{F}_9(h) = f_9 + \mathcal{O}(h)$ [34, 35], but the $\mathcal{O}(h)$ terms will be unnecessary unless processes with several Higgs bosons (or higher orders of perturbation theory) are addressed.

Just as we did for the Higgs potential $V(h)$, in the analysis in this paper we will assume that the counting of any NLO fermionic operators is suppressed by a power of the fermion mass. That couplings of the new scalar (Higgs) boson to fermions are indeed proportional to their masses is what phenomenological analysis seem to be suggesting, both directly from Higgs-related measurements [41] and from flavor-factory legacy.

[3] Of course, for analysis of the electroweak sector above 500 GeV only the top quark Yukawa might play some role, all the other ones being much more suppressed numerically.

JHEP03(2018)159

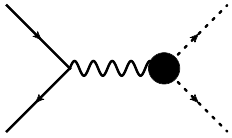

Figure 1. Tree-level Feynman diagram leading the production of Wh and Zh via the annihilation of $q\bar{q}'$ quarks into a gauge $W^{\pm}(Z)$ boson. Strong rescattering in the final state appears through the form factor $\mathcal{F}_A(s)$ represented by the thick blob.

3 The elementary subprocesses $q\overline{q'} \to W_L/Z_L + h$ at leading order

In this work we address the resonant production of $W^{\pm}h$ or Zh pairs at the LHC. At very high energies the corresponding cross sections are very small unless there is new physics, for example if it turns out that the spontaneous symmetry breaking of the SM is induced by new strong interactions. In that case the longitudinal components of the electroweak gauge bosons dominate the production and may have large enough cross sections to be detectable at the LHC through the subprocesses appearing in the title of this section. For the angular momentum J and custodial isospin I both equal to one, the corresponding amplitudes will be estimated with the Feynman diagram in figure 1.

In the limit when the light-quark Yukawas are negligible, the amplitude in figure 1 factorizes into the tree-level productions $q\overline{q'} \to W^* \to W_L h$ and $q\overline{q'} \to Z^* \to Z_L h$ and an axial form factor $\mathcal{F}_A(s)$ encoding the strong rescattering $V_L h$. For SISBS theories, this form factor is clearly of a non-perturbative nature. In this work, it will be computed by using the LO Electroweak Chiral Lagrangian of eq. (2.1) up to the one-loop level and the NLO Lagrangian (2.5) at tree-level, complemented with dispersion relations (unitarization of the amplitudes) and the Equivalence Theorem, as exposed next in sections 5 and 6.

At LO in the HEFT, the tree-level amplitudes of the quark-antiquark subprocesses (thus, not including any form factor yet), are given, in their center of mass (CM), by

$$T(u_-\bar{d}_+ \to W_L^+ h) = \frac{g^2}{\sqrt{2}} a V_{ud} \frac{\sqrt{s} E_W}{s - M_W^2} \sin\theta e^{-i\varphi} \tag{3.1}$$

$$T(d_-\bar{u}_+ \to W_L^- h) = \frac{g^2}{\sqrt{2}} a V_{ud}^* \frac{\sqrt{s} E_W}{s - M_W^2} \sin\theta e^{-i\varphi} \tag{3.2}$$

$$T(u_-\bar{u}_+ \to Z_L h) = \frac{e^2}{2 s_W^2 c_W^2} a \alpha_u \frac{\sqrt{s} E_Z}{s - M_Z^2} \sin\theta e^{-i\varphi} \tag{3.3}$$

$$T(d_-\bar{d}_+ \to Z_L h) = \frac{-e^2}{2 s_W^2 c_W^2} a \alpha_d \frac{\sqrt{s} E_Z}{s - M_Z^2} \sin\theta e^{-i\varphi} \tag{3.4}$$

$$T(u_+\bar{u}_- \to Z_L h) = \frac{-e^2}{2 s_W^2 c_W^2} a \beta_u \frac{\sqrt{s} E_Z}{s - M_Z^2} \sin\theta e^{i\varphi} \tag{3.5}$$

$$T(d_+\bar{d}_- \to Z_L h) = \frac{e^2}{2 s_W^2 c_W^2} a \beta_d \frac{\sqrt{s} E_Z}{s - M_Z^2} \sin\theta e^{i\varphi}, \tag{3.6}$$

where the $+$ and $-$ u and d (anti) quark subindices denote their helicity state and a is the first parameter of the $F(h)$ function appearing in the SISBS Lagrangian of eq. (2.1):

JHEP03(2018)159

$F(h) = 1 + 2ah/v + bh^2/v^2 + \mathcal{O}(h^3)$ (notice that in the SM $a = 1$, $b = a^2$; a separation thereof signals strong interactions). Furthermore, s_W and c_W are respectively the sine and cosine of the weack angle and

$$\begin{aligned} \alpha_u &= 1 - \frac{4}{3}s_W^2 \\ \alpha_d &= 1 - \frac{2}{3}s_W^2 \\ \beta_u &= -\frac{4}{3}s_W^2 \\ \beta_d &= -\frac{2}{3}s_W^2 \ . \end{aligned} \tag{3.7}$$

Finally E_W and E_Z are the energies of the produced W and Z gauge bosons and θ and φ are the corresponding polar and azimuthal CM scattering angles, respectively.

At the high energies in which we are interested here $\sqrt{s} \gg M_W, M_Z, M_h$, those amplitudes become:

$$T(u_-\bar{d}_+ \to W_L^+ h) = \frac{g^2}{2\sqrt{2}} a V_{ud} \sin\theta e^{-i\varphi} \tag{3.8}$$

$$T(d_-\bar{u}_+ \to W_L^- h) = \frac{g^2}{2\sqrt{2}} a V_{ud}^* \sin\theta e^{-i\varphi} \tag{3.9}$$

$$T(u_-\bar{u}_+ \to Z_L h) = \frac{g^2}{4c_W^2} a\alpha_u \sin\theta e^{-i\varphi} \tag{3.10}$$

$$T(d_-\bar{d}_+ \to Z_L h) = \frac{-g^2}{4c_W^2} a\alpha_d \sin\theta e^{-i\varphi} \tag{3.11}$$

$$T(u_+\bar{u}_- \to Z_L h) = \frac{-g^2}{4c_W^2} a\beta_u \sin\theta e^{i\varphi} \tag{3.12}$$

$$T(d_+\bar{d}_- \to Z_L h) = \frac{g^2}{4c_W^2} a\beta_d \sin\theta e^{i\varphi} \ . \tag{3.13}$$

Guided by the precision LEP observables, we assume that custodial $\mathrm{SU}(2)_{L+R}$ symmetry is a good approximation to the electroweak SISBS. This is obtained in the limit $g' = 0$ (which implies $s_W = 0$, $c_W = 1$ so that $\alpha_u = \alpha_d = 1$ and $\beta_u = \beta_d = 0$). As experimentally $|V_{ud}| \simeq 0.9758$, we will take $V_{ud} = 1$. In the following we will simplify the amplitudes of eq. (3.8) with that approximation. Then the non-vanishing ones are given by the simpler formulae

$$T(u_-\bar{d}_+ \to W_L^+ h) = T(d_-\bar{u}_+ \to W_L^- h) = \frac{g^2}{2\sqrt{2}} a \sin\theta e^{-i\varphi} \tag{3.14}$$

$$T(u_-\bar{u}_+ \to Z_L h) = -T(d_-\bar{d}_+ \to Z_L h) = \frac{g^2}{4} a \sin\theta e^{-i\varphi} \tag{3.15}$$

whereas, because $\beta_{u/d} \to 0$, $T(u_+\bar{u}_- \to Z_L h) = T(d_+\bar{d}_- \to Z_L h) = 0$.

In the presence of strong final state interactions, the amplitudes need to be modified by the introduction of an axial form factor $\mathcal{F}_A(s)$. Thus the complete results will have

JHEP03(2018)159

the form

$$\tilde{T}(u_-\bar{d}_+ \to W_L^+ h) = \tilde{T}(d_-\bar{u}_+ \to W_L^- h) = \frac{g^2}{2\sqrt{2}} a \sin\theta e^{-i\varphi} \mathcal{F}_A(s)\,,$$
$$\tilde{T}(u_-\bar{u}_+ \to Z_L h) = -\tilde{T}(d_-\bar{d}_+ \to Z_L h) = \frac{g^2}{4} a \sin\theta e^{-i\varphi} \mathcal{F}_A(s)\,. \tag{3.16}$$

The nonperturbative computation is thus isolated into computing the form factor $\mathcal{F}_A(s)$. Next, in section 4 we study in detail the $W_L h$ and $Z_L h$ interactions and show how axial resonances arise out of these interactions.

4 The strongly interacting $W_L h$ and $Z_L h$ amplitudes

In order to obtain the axial form factor that dresses the amplitudes in eq. (3.14) one needs to have at hand an appropriate and as general as possible a description of elastic $W_L h$ and $Z_L h$ scattering. Our approach here will start from the effective Electroweak Chiral Lagrangian in eqs. (2.1) and (2.5). Then we will use the Equivalence Theorem [1–5] as applied to this kind of Lagrangian [6–9]. The theorem relates the electroweak amplitudes (in renormalizable gauges) involving longitudinal components of the W and Z gauge bosons with the ones involving the corresponding would-be Goldstone bosons at high energies. In the case of interest here it reads (in the CM rest frame)

$$T\left(W_L^\pm(Z_L)h \to W_L^\pm(Z_L)h\right) = -T\left(\omega^\pm(\omega^0)h \to \omega^\pm(\omega^0)h\right) + \mathcal{O}\left(\frac{M_W}{\sqrt{s}}\right). \tag{4.1}$$

Therefore at high energies we can have access to the strongly interacting SBS of the SM by studying the elastic scattering of the longitudinal components of the W, Z and the Higgs boson h. While the gauge boson polarization is not yet systematically reconstructed at the LHC, it appears that it may become possible [42, 43]. If there are new strong interactions of the electroweak sector beyond the Standard Model, they enhance the $W_L W_L$ signal and make it more amenable to separate it from background. Additionally, the LHC will be rigged to operate at 10 times the current design luminosity after an upgrade, further increasing the number of events and facilitating the application of appropriate experimental cuts to eliminate background.

The amplitude for the would-be Goldstone (ω's) bosons and h can be computed at tree level from the Lagrangian in eq. (2.1) (order s). As this Lagrangian is not renormalizable, going to the one-loop level (oder s^2) requires the introduction of derivative counterterms depending on new couplings, as it is standard in chiral perturbation theory. Upon renormalization, these couplings absorb the one-loop divergences of the elastic amplitudes and pararametrize, in a systematic way, our ignorance about the underlying SISBS for these processes. Thus, up to NLO, the relevant scalar Lagrangian in spherical coordinates is

$$\begin{aligned}\mathcal{L} = &\frac{1}{2}\left(1 + 2a\frac{h}{v} + b\left(\frac{h}{v}\right)^2\right)\partial_\mu\omega^a\partial^\mu\omega^b\left(\delta_{ab} + \frac{\omega^a\omega^b}{v^2}\right) + \frac{1}{2}\partial_\mu h\partial^\mu h \\ &+\frac{4a_4}{v^4}\partial_\mu\omega^a\partial_\nu\omega^a\partial^\mu\omega^b\partial^\nu\omega^b + \frac{4a_5}{v^4}\partial_\mu\omega^a\partial^\mu\omega^a\partial_\nu\omega^b\partial^\nu\omega^b + \frac{g}{v^4}(\partial_\mu h\partial^\mu h)^2 \\ &+\frac{2d}{v^4}\partial_\mu h\partial^\mu h\partial_\nu\omega^a\partial^\nu\omega^a + \frac{2e}{v^4}\partial_\mu h\partial^\nu h\partial^\mu\omega^a\partial_\nu\omega^a\end{aligned} \tag{4.2}$$

JHEP03(2018)159

that we have described in detail in [44]. With this practical Lagrangian at hand we have computed the one-loop amplitudes for elastic processes involving Goldstone bosons and the Higgs. In the present application we provide the amplitude $\omega h \to \omega h$ given by

$$T_{II_z}(\omega^{I_z} h \to \omega^{I'_z} h) = M(s,t,u)\delta_{I_z I'_z} \tag{4.3}$$

where $I = 1$ is the $\mathrm{SU}(2)_{L+R}$ custodial isospin and s, t and u are the standard Mandelstam variables for massless particles since at high energies ($\sqrt{s} \gg M_h$) we will be neglecting the Higgs (and vector boson) mass in agreement with eq. (4.1). Then,

$$\begin{aligned} M(s,t,u) = & \frac{a^2-b}{v^2}t + \frac{2d^r(\mu)}{v^4}t^2 + \frac{e^r(\mu)}{v^4}(s^2+u^2) \\ & + \frac{a^2-b}{576\pi^2 v^4}\Bigg[\Bigg(72 - 88a^2 + 16b + 36(a^2-1)\log\frac{-t}{\mu^2} \\ & + 3(a^2-b)\left(\log\frac{-s}{\mu^2} + \log\frac{-u}{\mu^2}\right)\Bigg)t^2 \\ & + (a^2-b)\left(26 - 9\log\frac{-s}{\mu^2} - 3\log\frac{-u}{\mu^2}\right)s^2 \\ & + (a^2-b)\left(26 - 9\log\frac{-u}{\mu^2} - 3\log\frac{-s}{\mu^2}\right)u^2\Bigg] \end{aligned} \tag{4.4}$$

This can be obtained from our previously published [40, 44, 45] $\omega\omega \to hh$ amplitude by crossing. The renormalized couplings $d^r(\mu)$ and $e^r(\mu)$ depend on the renormalization scale μ as

$$\begin{aligned} d^r(\mu) &= d^r(\mu_0) + \frac{1}{192\pi^2}(a^2-b)\left[(a^2-b) - 6(1-a^2)\right]\log\frac{\mu^2}{\mu_0^2} \\ e^r(\mu) &= e^r(\mu_0) - \frac{1}{48\pi^2}(a^2-b)^2\log\frac{\mu^2}{\mu_0^2}\,. \end{aligned} \tag{4.5}$$

so that the amplitude in eq. (4.4) is μ invariant.

If a resonance of definite spin J appears dynamically or couples to $V_L h$ in any way, it should appear in the corresponding partial wave amplitudes. It is then convenient to compute the first few partial waves that dominate the amplitude of eq. (4.4) at low energy. The $I = J = 1$ partial wave needed for this work is given by

$$M_{11}(s) = \frac{1}{32\pi}\int_{-1}^{1} x\, M(s,t,u)\, dx \tag{4.6}$$

where $t = -s(1-x)/2$ and $u = -s(1+x)/2$. A direct computation of the integral shows that this partial wave adopts the generic form common to other scattering processes at NLO [36]:

$$M_{11}(s) = M_{11}^{(0)}(s) + M_{11}^{(1)}(s) = Ks + s^2\left[B(\mu) + D\log\frac{s}{\mu^2} + E\log\frac{-s}{\mu^2}\right]. \tag{4.7}$$

JHEP03(2018)159

where

$$
\begin{aligned}
K &= \frac{a^2-b}{96\pi v^2} \\
B(\mu) &= \frac{e^r(\mu)-2d^r(\mu)}{96\pi v^4} - \frac{a^2-b}{110592\pi^3 v^4}\left(150(1-a^2)-83(a^2-b)\right) \\
D &= \frac{a^2-b}{4608\pi^3 v^4}\left(3(1-a^2)-(a^2-b)\right) \\
E &= -\frac{(a^2-b)^2}{9216\pi^3 v^4}\ .
\end{aligned}
\tag{4.8}
$$

This axial-vector partial wave is defined in the whole complex s plane and it has the expected left cut (LC) along the negative real s-axis and the unitarity or right cut (RC) along the positive real s-axis. The physical amplitude is obtained by taking $s = E_{\rm CM}^2 + i0$, i.e. just over the RC, with $E_{\rm CM}$ being the total CM energy.

At low energies, phase space for channels with more particles suppresses inelastic amplitudes and elastic unitarity on the physical region is rather well satisfied, so that

$$
{\rm Im}M_{11}(s) = \mid M_{11}(s) \mid^2 \ . \tag{4.9}
$$

However the NLO amplitude in eq. (4.7) fulfills the unitarity condition at a perturbative level only,

$$
{\rm Im}M_{11}^{(1)}(s) = \mid M_{11}^{(0)}(s) \mid^2 \ . \tag{4.10}
$$

This is equivalent to the relation $E = -K^2/\pi$ among the constants of eq. (4.8), which can be very easily checked. The more demanding exact elastic unitarity condition of eq. (4.9) can be satisfied, with only the NLO computation at hand, by using, among other possibilities [44], the Inverse Amplitude Method (IAM [46–48]). According to it, the unitarized amplitude is given by

$$
\tilde{M}_{11}(s) = \frac{M_{11}^{(0)}(s)^2}{M_{11}^{(0)}(s) - M_{11}^{(1)}(s)}. \tag{4.11}
$$

This amplitude fulfills the exact elastic unitarity condition in eq. (4.9), it has the proper analytical structure (LC and RC), it is μ-independent and its low-energy expansion coincides with the HEFT up to the NLO:

$$
\tilde{M}_{11}(s) = M_{11}^{(0)}(s) + M_{11}^{(1)}(s) + O(s^3/v^6)\ . \tag{4.12}
$$

Moreover, for certain regions of the coupling space, this amplitude (4.11) can feature a pole at some point s_0 in the second Riemann sheet of the s complex plane. Any such poles have a natural interpretation as dynamically generated resonances with mass M and width Γ given by the relation $s_0 = M^2 - iM\Gamma$. The IAM method has been extensively and successfully applied to ordinary Chiral Perturbation Theory to describe pion and kaon scattering and the associated resonances $f(500)$, ρ and many others. Thus we may have some confidence that the method could work also in reproducing dynamical resonances in the context of the SISBS of the SM.

JHEP03(2018)159

Since the IAM formula is compact and simply algebraic, as opposed to the difficult integral expressions of usual dispersion relations, we can study the position of its complex s-plane poles (resonances) directly. In the case of axial resonances with mass M_A and relative small width Γ_A (so that $\gamma_A \equiv \Gamma_A/M_A \ll 1$) we find

$$M_A^2 = \frac{K}{B} = v^2 \frac{a^2-b}{e-2d+\frac{a^2-b}{1152\pi^2}[150(a^2-1)+83(a^2-b)]} \tag{4.13}$$

$$\gamma_A = \frac{K^2}{B+D+E} = \frac{\gamma_A^0}{1-\frac{3}{\pi}\gamma_A^0\left(1+2\frac{a^2-1}{a^2-b}\right)} \tag{4.14}$$

where

$$\Gamma_A^0 = M_A\gamma_A^0 = \frac{a^2-b}{96\pi v^2}M_A^3 \tag{4.15}$$

and the $d(\mu)$ and $e(\mu)$ couplings (from now on we will drop the superscript r in the renormalized couplings) are evaluated at $\mu = M_A$ (it is necessary to state this since $d-2e$ is not, in general, renormalization-scale invariant). Obviously the region of parameters a, b, d and e yielding a dynamical axial resonance is defined as the region $M_A^2 > 0$ (though below about 500 GeV our use of the Equivalence Theorem does not hold scrutiny anymore) and $\gamma_A > 0$.

Equation (4.13) shows that the LO parameters alone (that is, $d = e = 0$ but $a^2 - b \neq 0$) are sufficient to generate an axial resonance. This is generically broad, as the width is proportional to the same $(a^2 - b)$ separation from the SM. In the limit $b \to a^2$ fulfilled by dilatonic theories [49, 50] and the SM, the axial-vector becomes narrow, $\gamma_A \to 0$, and gets a mass $M_A^2 = 192\pi^2 v^2/[25(a^2-1)]$, implying $a > 1$. Likewise, one gets the lower bound $M_A > 3.6\,\text{TeV}$ for $a < 1.16$. In the SM ($a \to 1$), this mass goes to infinity, decoupling from the low-energy theory. Such resonances are generically called "dynamically generated" and it is unclear whether they correspond to a new particle or field that should enter a fundamental Lagrangian, depending on how broad the width is. The textbook example of this behavior is the $f_0(500)$ or σ-meson in hadron physics.

On the other hand, the NLO coefficients e or d can yield a light resonance, as they suppress the numerator in eq. (4.13). The resonance is then narrower, as eq. (4.15) shows a kind of KSFR relation: the width is proportional to the cube of the mass times a known combination of the coefficients that does not depend on d, e. Very often one expects that a resonance dominated by the NLO Lagrangian terms is actually a physical particle, and there is ample work integrating out that high energy field from the underlying action to yield expressions for the EFT coefficients in terms of its properties.

Figures 2, 3 and 4 illustrate the resonances obtained in various cases of interest, depending on the Lagrangian parameters. These amplitudes only depend on the combination $e(\mu) - 2d(\mu)$, so we have fixed $d(\mu) = 0$ and varied $e(\mu)$ in all the plots.

The method can accommodate a variety of resonances (or none). Nevertheless, being based on an underlying Lagrangian, once its parameters are measured it does have predictive power yielding a specific spectrum and scattering amplitudes at higher energies. Some works [51, 52] have tried to assess the reliability of the Inverse Amplitude Method

JHEP03(2018)159

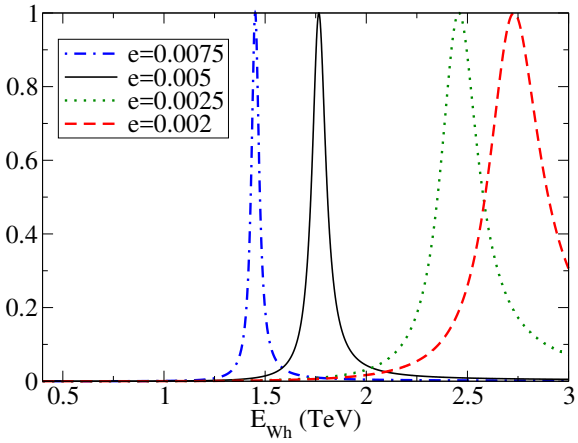

Figure 2. The $I = J = 1$ axial resonance generated in $V_L h$ scattering by the e counterterm in the NLO HEFT Lagrangian, with values of the constant at $\mu = 3\,\text{TeV}$ as indicated in the legend. Here, $d = 0$, $a = 0.95$ and $b = 0.7a^2$ are fixed.

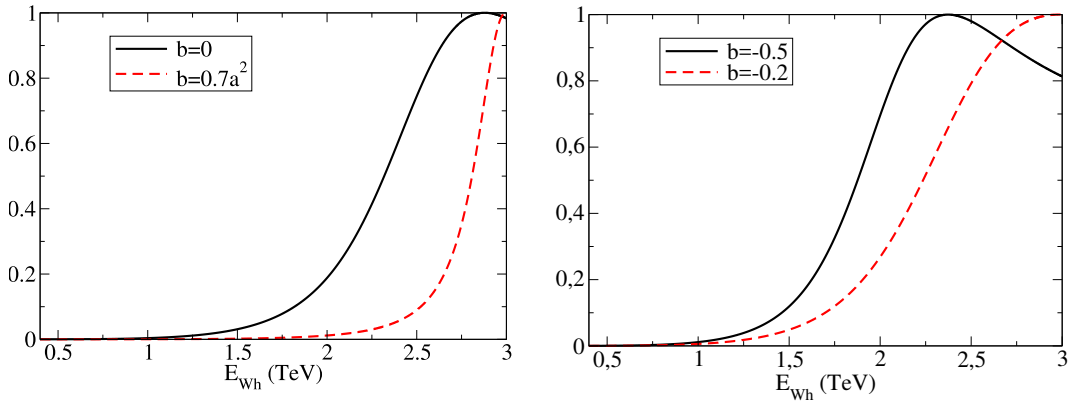

Figure 3. The $I = J = 1$ axial resonance generated in $V_L h$ scattering. Here we show the dependence on b, with a fixed (on the left plot, to 0.95, on the right to -0.9) as well as fixing e (to 1.64×10^{-3} on the left plot, to 0 on the right). In both cases $d = 0$.

in the past. Therein, a scalar resonance was coupled and then integrated out from the EFT so its effect was only felt in the coefficients of the NLO Lagrangian. The IAM was then applied to the resulting Lagrangian, and indeed a resonance of the $W_L W_L$ subsystem was generated, with equal quantum numbers and a mass close to the original one (though different width). Thus, although the unitarization procedure brings on some theoretical uncertainties, the predictions of the present exploratory analysis are robust enough, as we are just providing a first estimate of the WZ resonant production cross section within the EW chiral framework. A precise determination requires further studies (mass effects, top loops, experimental cuts and efficiencies, etc.) which are out of the scope of this article. In addition, the predictive power of the IAM has been extensively checked in low-energy hadron physics: in this case the low-energy EFT is Chiral Pertubation Theory, which complemented with the IAM is able to describe many hadronic resonances [46–48, 53].

JHEP03(2018)159

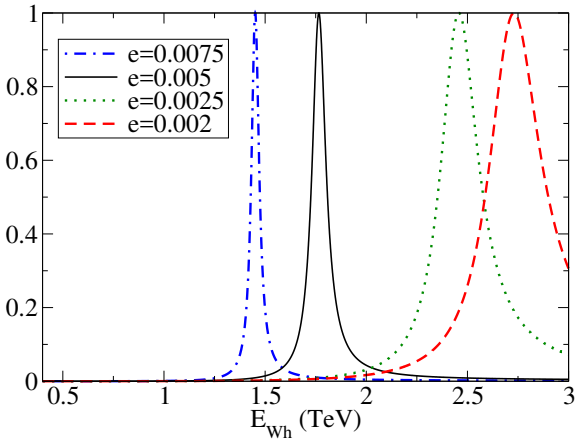

Figure 4. The $I = J = 1$ axial resonance generated in $V_L h$ scattering with $a = 0.95$. Here we have fixed $2a^2 - b = 1$ which is a characteristic prediction of Minimally CHM. We set $d = 0$.

5 The axial-vector form factor up to NLO in HEFT

The piece connecting the Strongly Interacting Sector described in section 4 with its perturbative coupling to the fermions of the Standard Model as in section 3 is the axial form factor $\mathcal{F}_A(q^2)$ in the ωh sector that dresses the $V^* \to V_L h$ vertex. In this section we quickly compute it in perturbation theory, and defer to more sophisticated treatment necessary to address resonances for the next section.

In our treatment of the low-energy HEFT, the necessary operators at lowest order are provided by eq. (2.1) and those at next-to-leading order by eq. (2.5). In particular, in the ET limit the Axial Form Factor (AFF) only depends on one NLO effective coupling, f_9. At NLO in this limit this operator absorbs the ultraviolet divergences cause by the one-lop AFF diagrams built out of the LO vertices from (2.1). In respecting custodial symmetry, the neutral-current form factor is provided by an isospin rotation and coincides with the charged one.

The computation of the ωh AFF $\mathcal{F}_A(q^2)$ proceeds by extracting the kinematic factors from the matrix element

$$\langle\, \omega^-(p_1)\, h(p_2) | J_A^\alpha | 0 \,\rangle \;=\; (-i\sqrt{2}\, a)\, \mathcal{F}_A(q^2)\; P_T(q)^{\alpha\beta} (p_1 - p_2)_\beta \,, \tag{5.1}$$

with $q = p_1 + p_2$, $s = q^2$ in the timelike region for our application, and the $L - R$ charged current being $J_A^\alpha = \frac{\delta S}{\delta a_\alpha}$ (with $a_\alpha = g W_\alpha^+/(2\sqrt{2})$ in the SM). In practice this means that the vertex function for $W_\alpha^- \to \omega^- h$ with external on-shell ω^- and h (but W^- off-shell) is equal to

$$i \frac{a\, g}{2\sqrt{2}} \times (-i\sqrt{2})\, \mathcal{F}_A(s)\, P_T(q)^{\alpha\beta} (p_1 - p_2)_\beta \,. \tag{5.2}$$

The normalization of the AFF defined in eq. (5.1) at zero momentum transfer is $\mathcal{F}_A(0) = 1$, in consistency with the definition employed in previous sections. To achieve this, a factor a has been explicitly factorized out (other works [27, 28] include this a factor within $\mathcal{F}_A(s)$ instead).

JHEP03(2018)159

Within the ET and neglecting once more the Higgs and W and Z masses at energies high enough over the Wh threshold one obtains the low-energy effective theory prediction for the AFF up to NLO,

$$\mathcal{F}_A(s) = \mathcal{F}_A^{(0)}(s) + \mathcal{F}_A^{(1)}(s) + \dots \tag{5.3}$$

where

$$\begin{aligned} \mathcal{F}_A^{(0)}(s) &= 1 \\ \mathcal{F}_A^{(1)}(s) &= s\left(G(\mu) + H\ln\frac{-s}{\mu^2}\right), \end{aligned} \tag{5.4}$$

in a notation analogous to eq. (4.7)

$$\begin{aligned} G(\mu) &= -\frac{f_9(\mu)}{a\,v^2} + \frac{(a^2-b)}{36\pi^2 v^2}, \\ H &= -\frac{(a^2-b)}{96\pi^2 v^2}. \end{aligned} \tag{5.5}$$

The NLO effective coupling f_9 renormalizes the one-loop divergence (here in the $\overline{MS}$ scheme in dimensional regularization) and runs with the scale in the form

$$f_9(\mu) = f_9(\mu_0) + \frac{a\,(a^2-b)}{96\pi^2}\log\frac{\mu^2}{\mu_0^2} \tag{5.6}$$

such that $\mathcal{F}_A(s)$ is μ independent and in agreement with the path integral renormalization in [54] (with notation $f_9 = c_9(0) = \mathcal{F}_9(0)$ therein).

The EFT result from eq. (5.4) and (5.5) does not depend on whether the Goldstone field U(ω) is parametrized in spherical, exponential, or any other coordinates. This satisfying feature happens, in the ($s \gg M_h, M_W, M_Z \to 0$) approximation because the four LO vertices active in the computation ($W\omega h$, $W\omega$, $h\omega\omega$ and $hh\omega\omega$) and the one NLO vertex ($W\omega h$) all have at most two Goldstone fields each.

The AFF from eq. (5.4) and (5.5) is an analytical function in the whole complex s-plane but for a RC, as expected. On the other hand, in the elastic regime, unitarity relates the imaginary part of the axial form factor with the partial-wave scattering amplitude $M_{11}(s)$ in the form

$$\mathrm{Im}\mathcal{F}_A(s) = \mathcal{F}_A(s)\,M_{11}(s)^*. \tag{5.7}$$

However the one-loop result only fulfills this relation at the perturbative level -i.e., up to NLO in the low-energy expansion–:

$$\mathrm{Im}\mathcal{F}_A^{(1)}(s) = \mathcal{F}_A^{(0)}(s)\,M_{11}^{(0)}(s)^* = M_{11}^{(0)}(s), \tag{5.8}$$

where on the last step we have used that $\mathcal{F}_A^{(0)}(s) = 1$ and that the tree-level amplitude $M_{11}(s)$ is real. This is easy to check comparing eq. (5.5) and (4.8), which satisfy $H = -K/\pi$. The reason of the violation of (exact) unitarity in the EFT calculation is the absence of higher order corrections. As far as energies remain small enough these deviations are negligible and our effective theory provides an appropriate approximation of the physical amplitude.

JHEP03(2018)159

6 The axial form factor in the resonance region

In this section we address the problem of how to obtain an appropriate AFF $\mathcal{F}_A(s)$ to describe the W_Lh and Z_Lh resonant production at the LHC. We deploy four different methods and show that, for relatively narrow resonances, all give very similar results.

6.1 AFF with a resonance Lagrangian

The simplest approach, often employed by experimental collaborations in the search for new particles, is to include the resonance field explicitly as a degree of freedom in a resonance Lagrangian $\mathcal{L}_R$ [28, 35]. At tree-level, one finds a Breit-Wigner like formula

$$\begin{aligned}\mathcal{F}_A(s) &= 1 + \frac{F_A\lambda_1^{hA}}{a\,v}\frac{s}{M_A^2 - s} \\ &= 1 + \frac{s}{M_A^2 - s}\,,\end{aligned} \tag{6.1}$$

where the F_A and λ_1^{hA} constants are respectively the $W \to A$ and $A \to \omega h$ vertex couplings; in the last identity, they are fixed by [28, 35]

$$F_A\lambda_1^{hA} \;=\; a\,v \tag{6.2}$$

upon demanding that the AFF vanishes at asymptotically high energy (this depends on the underlying theory, and is typical, for example, of a non-Abelian gauge Lagrangian which yields asymptotic freedom).

Expanding the AFF (6.1) in powers of the squared four-momentum s one obtains the tree-level matching condition $f_9 = -F_A\lambda_1^{ha}v/M_A^2 = -av^2/M_A^2$, in agreement with previous works [35].

The intermediate resonance need not be infinitesimally narrow and its width Γ_A can be taken into account easily (which makes the form-factor regular on the real axis), yielding the relativistic Breit-Wigner line shape,

$$\mathcal{F}_A(s) \;=\; 1 \;+\; \frac{s}{M_A^2 - iM_A\Gamma_A - s}\,. \qquad \text{(Model I)} \tag{6.3}$$

In principle Γ_A is an independent parameter. Nevertheless, if the presumed ωh resonance is very elastic, suppressing other decay channels, the λ_1^{ha} coupling of the resonance Lagrangian governs the width directly via

$$\Gamma_A = \frac{\lambda_1^{hA}M_A^3}{48\pi v^2} \;=\; \frac{a^2M_A^3}{48\pi F_A^2}\,, \tag{6.4}$$

where the $W \to A$ coupling F_A is expected to be of $\mathcal{O}(v)$.

Adding the experimental constraints from the oblique S and T parameters, further reduces the number of parameters. For instance, under the assumption that the W^3B correlator obeys two Weinberg sum-rules dominated by the lightest vector and axial-vector resonances [28], the axial-vector width becomes

$$\Gamma_A = a(1-a)\frac{M_A^3}{48\pi v^2}\,. \tag{6.5}$$

JHEP03(2018)159

Thus, for instance, a $M_A = 3\,\text{TeV}$ resonance would have a width $\Gamma_A < 140\,\text{GeV}$ for $0.95 < a < 1$. A noticeable feature of eq. (6.5) is the absence of the ubiquitous factor $(a^2 - b)$ — compare it, for example, with eq. (4.15) —. The reason is that the underlying effective Lagrangian including resonances explicitly correlates a and b, so there is one less parameter.

Obviously, in less constrained scenarios where some of the previous theoretical assumptions are relaxed, one could obtain broader resonances. But masses of a few TeV and widths of a few hundred GeV naturally appear in HEFT frameworks if the underlying theory is taken to be QCD-like.

In the next subsection 6.2, we avoid introducing the resonance as an explicit degree of freedom affecting $\mathcal{F}_A(s)$ and instead study it from analyticity and unitarization of the low-energy HEFT amplitude.

6.2 Unitarized HEFT parametrizations of the axial form factor

Ideally, a fully realistic axial form factor $\mathcal{F}_A(s)$ would have the following properties:

a Analiticity in the complex s plane, featuring just a right cut for physical s. (We already know empirically that there are no bound state poles below threshold in the 100-GeV spectrum).

b Coincidence of any resonance poles (in the second Riemann sheet) with those of the elastic amplitude $M_{11}(s)$.

c Elastic unitarity, i.e., $\mathcal{F}_A$ should fulfill eq. (5.7), while $M_{11}(s)$ satisfies eq. (4.9).

d Low-energy behavior that reproduces the chiral expansion $\mathcal{F}_A(s) = \mathcal{F}_A^{(0)}(s) + \mathcal{F}_A^{(1)}(s) + O(s^2/v^4)$.

Model I in eq. (6.3) features a resonance as in (b) and can be matched to the low-energy expansion (d), but has no cut and bears no ressemblance to the elastic amplitude, so that (a), (c) and most of (b) fail to be satisfied.

An alternative [55] would be to build a form factor from a Lippman-Schwinger like resummation of the perturbative form factor expansion,

$$\begin{aligned} \mathcal{F}_A(s) &= \frac{(\mathcal{F}_A^{(0)}(s))^2}{\mathcal{F}_A^{(0)}(s) - \mathcal{F}_A^{(1)}(s)} = 1 + \frac{\mathcal{F}_A^{(1)}(s)}{1 - \mathcal{F}_A^{(1)}(s)} \\ &= \frac{1}{1 - \mathcal{F}_A^{(1)}(s)}\,, \qquad \text{(Model II)} \end{aligned} \tag{6.6}$$

which inherits from $\mathcal{F}_A^{(1)}(s)$ the correct right cut, satisfying (a) and, by construction, (d), but is again unconnected to the elastic amplitude, so it fails to fulfill (b) and (c).

JHEP03(2018)159

From the elastic amplitude alone it is possible to build another form factor model [56–59] that satisfies (b) and (c)

$$\begin{aligned}\mathcal{F}_A(s) &= 1 + \frac{M_{11}^{(1)}(s)}{M_{11}^{(0)}(s) - M_{11}^{(1)}(s)} \\ &= \frac{1}{1 - \frac{M_{11}^{(1)}(s)}{M_{11}^{(0)}(s)}}\,, \qquad \text{(Model III)}\end{aligned} \tag{6.7}$$

but, having no knowledge of f_9, which is in principle independent, fails (d); and since $M_{11}^{(1)}$ has a left cut, it fails also (a) (while this feature is probably not severe if employed in the resonance region only, from which that spurious left cut is very far in the complex s-plane).

One can improve eq. (6.7) by correcting for the low energy expansion, introducing $\mathcal{F}_A^{(1)}$ as follows,

$$\mathcal{F}_A(s) = 1 + \frac{\mathcal{F}_A^{(1)}(s) M_{11}^{(0)}(s)}{M_{11}^{(0)}(s) - M_{11}^{(1)}(s)}\,. \qquad \text{(Model IV)} \tag{6.8}$$

This form factor satisfies all of (b), (c) and (d). The only problem left is that, together with the RC, it has also a LC from $M_{11}^{(1)}(s)$. But again, this LC is not expected to have a very strong influence in the physical timelike-s region (the RC) particularly in the TeV, perhaps resonant, range of energies.

Interestingly, all three form factors in models II–IV, eq. (6.6), (6.7), (6.8) would coincide if $M_{11}^{(1)}(s) = \mathcal{F}_A^{(1)}(s) M_{11}^{(0)}(s)$. This boils down to the following relations among the coefficients of $M_{11}^{(1)}(s)$ and those of $\mathcal{F}_A^{(1)}(s)$,

$$D = 0\,, \tag{6.9}$$

$$E = KH\,, \tag{6.10}$$

$$B(\mu) = KG(\mu)\,. \tag{6.11}$$

The first condition is equivalent to neglecting the LC contribution and it is fulfilled for $b = a^2$ (as in the SM) or $b = 4a^2 - 3$. The second identity is always obeyed, since it is a consequence of perturbative unitarity. The last one imposes a relation between $f_9(\mu)$ and the rest of the couplings so it can be fulfilled by a proper election of this parameter as a function of those in the Lagrangian of eq. (2.5), namely a, b and the combination $e(\mu) - 2d(\mu)$.

In general this choice of the parameter f_9 appears to be possible only at a given scale, so it would be μ dependent; however, if eqs. (6.9) and (6.10) are obeyed then the right-hand and left-hand sides of eq. (6.11) have exactly the same running and all choices of μ are equivalent; the appropriate choice of f_9 is

$$\frac{f_9}{a} = \frac{50(1-a^2) - 17(a^2 - b)}{384\pi^2} + \frac{2d - e}{a^2 - b}\,. \tag{6.12}$$

In figure 5 we plot all four factor models $(I - IV)$ for a relatively narrow resonance in the neighbourhood of 3 TeV (this is achieved by appropriately setting either f_9 or $(e-2d)$,

JHEP03(2018)159

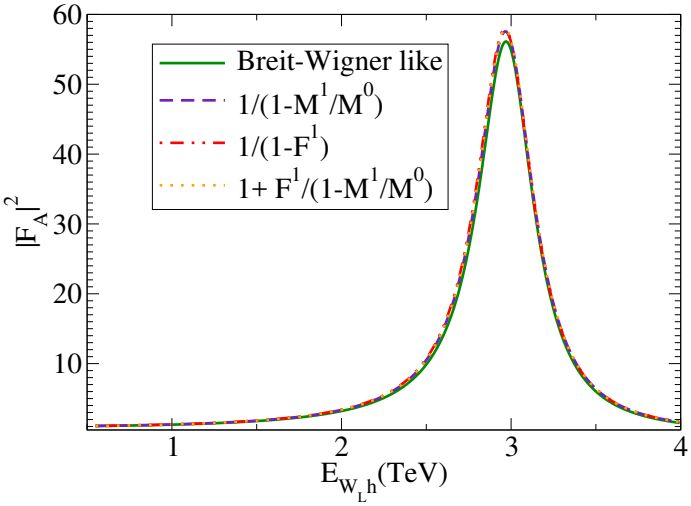

Figure 5. The $I = J = 1$ axial form factor in $V_L h$. Here we compare various models of the form factor for fixed values of the chiral parameters. Because the resonance is relatively narrow, the form factor is controlled by its physical mass and width parameters, so the model differences are small (at the level of a percent).

	Model	Eq. in text	Parameters
I	($\mathcal{L}_R$ Breit-Wigner like)	(6.3)	M_A, Γ_A
II	(Lipmann-Schwinger on pert. AFF)	(6.6)	$(a^2 - b)$, f_9/a
III	(From elastic IAM only)	(6.7)	a, b, $(e - 2d)$
IV	(Combined pert. AFF + IAM)	(6.8)	a, b, f_9, $(e - 2d)$

Table 1. Parameters employed to obtain the axial form factor of a relatively narrow $V_L h$ resonance with mass around 3 TeV and width about 0.5 TeV, plotted in figure 5.

depending on the model, see table 1). The agreement among them is spectacular (a consequence of the resonance being relatively narrow, so that the amplitude is pole-dominated) and therefore, it does not really matter what form factor model is used.

If one wants a quick cross-section estimate, the Breit-Wigner model (I) can as well be used; to use experimental data to constrain low-energy parameters of HEFT, the others should be implemented.

7 Cross section from intermediate gauge boson production

Now we are in a condition to provide a quick estimate for the resonant production of Wh and Zh at the LHC. After this extensive discussion, all pieces that enter the cross-section are at hand. For example we have, for the unpolarized CM cross-section,

$$\begin{aligned}\frac{d\hat{\sigma}(u\bar{d} \to W^+ h)}{d\Omega_{CM}} &= \frac{a^2}{64\pi^2 s}\left(\frac{1}{4}\right)\left(\frac{g^4}{8}\right) \mid \mathcal{F}_A(s) \mid^2 \sin^2\theta \\ &= a^2\,\frac{1}{128\,s}\,\frac{\alpha^2}{s_W^4}\,|\mathcal{F}_A(s)|^2\,\sin^2\theta\,. \end{aligned} \tag{7.1}$$

JHEP03(2018)159

Integrating over the full solid angle, one obtains

$$\hat{\sigma}(u\bar{d} \to W^+h) = a^2 \frac{\pi}{48s} \frac{\alpha^2}{s_W^4} \mid \mathcal{F}_A(s) \mid^2 \quad . \tag{7.2}$$

The strongly interacting SBS dynamics is encoded in the form factor which can be resonant or not depending on the parameters of the effective Lagrangian. If CP is conserved by the SISBS (as in our HEFT calculation up to NLO), the same formula provides $\sigma(d\bar{u} \to W_L^- h)$. Likewise, the $\sigma(q\bar{q} \to Z_L h)$ production cross section is given by eqs. (7.1) and (7.2) times a multiplicative factor $(\alpha_q^2 + \beta_q^2)/2$, and multiplied by the appropriate distribution functions and summed on $q = u, d$ for the production from pp collisions.

Convoluting eq. (7.2) with the parton distribution functions (which we take from the CJ (CTEQ-Jefferson Laboratory) set [60], that includes nuclear corrections, important at high x and thus at the energy frontier of the LHC, as well as Q^2 corrections), we obtain the proton-proton level inclusive cross-section to produce a $W_L h$ or $Z_L h$ pair (by using the corresponding amplitudes given above) as:

$$\begin{aligned}
\frac{d\sigma}{ds}(pp \to W_L^+ h + X) &= \int_{\frac{s}{E_{\rm tot}^2}}^1 \frac{dx_u}{x_u E_{\rm tot}^2} \hat{\sigma}_{u\bar{d}\to W_L^+ h}(s) F_{p/u}(x_u) F_{p/\bar{d}}(x_{\bar{d}}) \\
\frac{d\sigma}{ds}(pp \to W_L^- h + X) &= \int_{\frac{s}{E_{\rm tot}^2}}^1 \frac{dx_d}{x_d E_{\rm tot}^2} \hat{\sigma}_{d\bar{u}\to W_L^- h}(s) F_{p/d}(x_d) F_{p/\bar{u}}(x_{\bar{u}}) \,,
\end{aligned} \tag{7.3}$$

with $x_{\bar{d}} = s/(x_u E_{\rm tot}^2)$ and $x_{\bar{u}} = s/(x_d E_{\rm tot}^2)$. Here, s is the CM squared energy of the Wh pair, while $E_{\rm tot}$ is the CM energy of the pp LHC accelerator. A similar expression can be derived for the $Z_L h$ production, which provides a cross section of a similar order of magnitude and will not be studied in this exploratory work. For the example cross-section plotted in figure 6, we have set $E_{\rm tot}$ at 13 TeV. There, a resonance of mass 3 TeV and width 0.4 TeV has been injected with two of the form factors from figure 5. The LO parameters are $a = 0.95$, $b = 0.7a^2$ (away from their SM values $a = b = 1$), and the NLO ones $e(\mu) - 2d(\mu) = 1.64 \times 10^{-3}$ and $f_9(\mu) = -0.6 \times 10^{-2}$ for $\mu = 3$ TeV.[4]

Since the resonances here analyzed are native of the $W_L h$ EW SBS, they are rather elastic and the branching fraction $R \to W_L h$ is not too far below 1 and the difference therefrom can be ignored in a first experimental analysis (unlike other types of new physics that are weakly coupled to this channel).

We do find small cross-sections (fractions of a femtobarn) that are well below the current CMS and ATLAS cross-section upper bounds. The experimental collaborations are constraining W' and Z' models where the new resonance couples directly with charges $g_V = 1$ and $g_V = 3$, leading to femtobarn-size cross-sections. On the other hand, our computations proceed by the diagram of figure (1) with an intermediate W_T gauge boson and are smaller by a factor $(g/g_V)^4$. This means that it will be arduous for the LHC to

[4]This $f_9 = -6 \times 10^{-3}$, which leads to $M_A = 3$ TeV and $\Gamma_A = 0.4$ TeV, is very close to the value one would obtain from $e - 2d$ through (6.12), $f_9 = -5.6 \times 10^{-3}$. The proximity of this two values relies on the fact that both expressions lead to the same resonance pole and the conditions from (6.9)–(6.11) for BSM theories, $b = 4a^2 - 3 = 0.61$, is approximately fulfilled by our benchmark point $b = 0.7a^2 = 0.63$.

JHEP03(2018)159

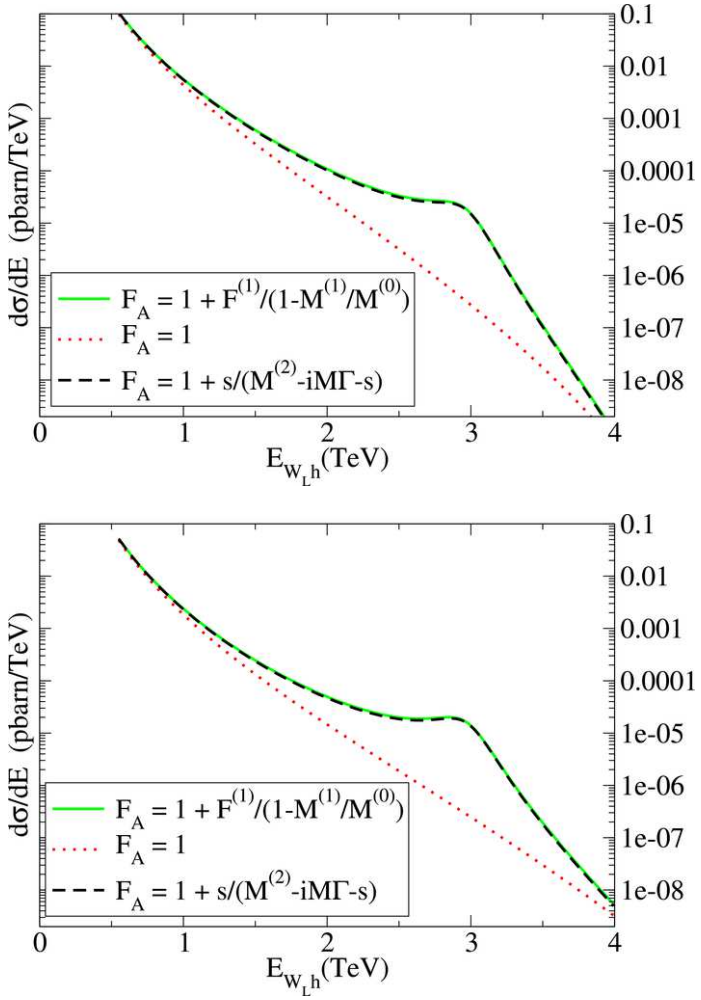

Figure 6. Production cross section of $W_L^{\pm}h$ pairs with (top solid green and dashed black lines) and without (bottom dotted red line) a 3 TeV axial-vector resonance. The cross-section is enhanced by the latter, in this case by over an order of magnitude. The top plot corresponds to W^+h and the bottom one to W^-h; they are almost equal near the peak, with the positively charged one dominating for small s_{Wh} and the negatively charged one at higher energy. Indeed, if we set the $\mathcal{F}_A(s)$ form factor to 1 (dotted red lines), the two cross-sections are very similar in the 3 TeV region.

fully constrain the "natural" parameter space in the 3 TeV region. For this reason, we look forward to its high-luminosity upgrade.

8 Conclusions

The IAM has been applied in this article to describe the strong elastic V_Lh rescattering in the regime where the ET applies ($s \gg M_W^2, M_Z^2, M_h^2$) that is, for energies above about 500 GeV, and, at the same time, an EFT description in terms of the low energy degrees of freedom makes sense ($s \ll (4\pi f)^2$, with f the vev scale of spontaneous symmetry breaking in the strong BSM sector).

JHEP03(2018)159

Notice again that we are neglecting masses and CKM mixing for this exploratory study. Clearly, a more exhaustive analysis should take into account the detector acceptance and appropriate kinematical cuts in the angular integration. Likewise, the W and h are not directly detected, but rather their decay products. Nevertheless, this type of 'realistic' analysis is out of the scope of this article and is relegated to future studies.

If the precision program of the LHC measures deviations from the SM in the low energy coefficients of the chiral Lagrangian (the relevant combinations of a, b, d and e for this work) EFT-based approaches can predict whether there is new physics within reach of the LHC. These methods are sufficiently robust to qualitatively predict whether there is a reasonable hope of detecting new physics resonances within the accelerator's energy reach, through equation (4.13). In our case, the axial-vector resonance mass and width and the low-energy parameters are constrained through the KSFR-like relation in eq. (4.15).

If other unitarization methods such as the N/D or the (improved) K-matrix method are employed, the results are consistent, and the theoretical method-choice uncertainty is about 20% in the determination of the resonance mass, as it was recently shown in [44]. One generically expects this from any unitarization method that respects analyticity in the complex plane. To reproduce an analytic function in its entire domain of analyticity (for example, a scattering amplitude in the resonance region) it is enough to know it with enough precision in a finite segment (for example, where the LHC can measure the low-energy coefficients) and to provide an appropriate analytical extension. Thus, unitary and analytic methods do have some predictive power. On the contrary, methods such as the old K-matrix are unitary but lack the right analytic structure, being less reliable.

Thus, we maintain that the combination of analyticity and unitarity can be helpful in constraining new physics once (if) the low-energy coefficients of the EFT are measured to separate from the Standard Model, if this new physics manifests itself as new strong interactions. This may happen through a clear, recognizable resonance or through strong scattering phase shifts with a pole deep in the complex s-plane. In both cases, the unitarization methods that we deploy make useful qualitative (and often also quantitative) statements as is well known from QCD theory. One should however not use the method to overpredict: unnaturally narrow resonances, a second resonance in each J^P channel, or the opening of new quasi-Goldstone boson thresholds (and generally any weakly coupled physics) are all very difficult to reproduce or predict.

Finally, it is worth remarking that our strongly interacting SBS analysis with chiral NLO couplings ($e-2d$ and f_9 here) of the order of 10^{-3} leads to much smaller production cross sections than those tested by the ATLAS and CMS Collaborations nowadays [61, 62]. This naturally allows the presence of resonances with mass $M_A \lesssim 3\,\text{TeV}$, while evading standing experimental bounds in Vh resonant production, contrary to some of the theoretical models considered by the experimental collaborations. An analogous study on WZ production within this same EW chiral framework [13] yields similar conclusions: chiral NLO couplings of order 10^{-3} lead to vector resonances with $M_V \sim 1$–$3\,\text{TeV}$ and a much lower production cross section than the current LHC sensitivity bounds. However, these EW chiral resonances in the few-TeV range could be accessible to future high-luminosity LHC runs with an expected integrated luminosity of the order of $3000\,\text{fb}^{-1}$.

JHEP03(2018)159

Acknowledgments

The authors thank Rafael L. Delgado for assistance and valuable comments at early stages of this investigation. We also want to thank C. García, M.J. Herrero and D. Espriu for useful comments and suggestions, and the members of UPARCOS for maintaining a stimulating intellectual atmosphere. Work supported by Spanish grants MINECO:FPA2014-53375-C2-1-P, FPA2016-75654-C2-1-P and the COST Action CA16108.

References

[1] J.M. Cornwall, D.N. Levin and G. Tiktopoulos, *Derivation of Gauge Invariance from High-Energy Unitarity Bounds on the s Matrix*, *Phys. Rev.* **D 10** (1974) 1145 [*Erratum ibid.* **D 11** (1975) 972] [INSPIRE].

[2] C.E. Vayonakis, *Born Helicity Amplitudes and Cross-Sections in Nonabelian Gauge Theories*, *Lett. Nuovo Cim.* **17** (1976) 383 [INSPIRE].

[3] B.W. Lee, C. Quigg and H.B. Thacker, *Weak Interactions at Very High-Energies: The Role of the Higgs Boson Mass*, *Phys. Rev.* **D 16** (1977) 1519 [INSPIRE].

[4] M.S. Chanowitz and M.K. Gaillard, *The TeV Physics of Strongly Interacting W's and Z's*, *Nucl. Phys.* **B 261** (1985) 379 [INSPIRE].

[5] G.J. Gounaris, R. Kogerler and H. Neufeld, *Relationship Between Longitudinally Polarized Vector Bosons and their Unphysical Scalar Partners*, *Phys. Rev.* **D 34** (1986) 3257 [INSPIRE].

[6] A. Dobado and J.R. Peláez, *On The Equivalence theorem in the chiral perturbation theory description of the symmetry breaking sector of the standard model*, *Nucl. Phys.* **B 425** (1994) 110 [*Erratum ibid.* **B 434** (1995) 475] [hep-ph/9401202] [INSPIRE].

[7] A. Dobado and J.R. Pelaez, *The Equivalence theorem for chiral lagrangians*, *Phys. Lett.* **B 329** (1994) 469 [hep-ph/9404239] [INSPIRE].

[8] C. Grosse-Knetter and I. Kuss, *The Equivalence theorem and effective Lagrangians*, *Z. Phys.* **C 66** (1995) 95 [hep-ph/9403291] [INSPIRE].

[9] H.-J. He, Y.-P. Kuang and X.-y. Li, *Proof of the equivalence theorem in the chiral Lagrangian formalism*, *Phys. Lett.* **B 329** (1994) 278 [hep-ph/9403283] [INSPIRE].

[10] LHC Higgs Cross Section Working Group collaboration, *Handbook of LHC Higgs Cross Sections: 4. Deciphering the Nature of the Higgs Sector*, arXiv:1610.07922 [INSPIRE].

[11] J.J. Sanz-Cillero, *Resonances and loops: scale interplay in the Higgs effective field theory*, in *2017 European Physical Society Conference on High Energy Physics (EPS-HEP 2017) Venice, Italy, July 5-12, 2017*, 2017, arXiv:1710.07611, http://inspirehep.net/record/1631815/files/arXiv:1710.07611.pdf [INSPIRE].

[12] A. Castillo, R.L. Delgado, A. Dobado and F.J. Llanes-Estrada, *Top–antitop production from $W_L^+W_L^-$ and Z_LZ_L scattering under a strongly interacting symmetry-breaking sector*, *Eur. Phys. J.* **C 77** (2017) 436 [arXiv:1607.01158] [INSPIRE].

JHEP03(2018)159

[13] R.L. Delgado et al., *Production of vector resonances at the LHC via WZ-scattering: a unitarized EChL analysis*, *JHEP* **11** (2017) 098 [arXiv:1707.04580] [INSPIRE].

[14] R. Alonso, M.B. Gavela, L. Merlo, S. Rigolin and J. Yepes, *The Effective Chiral Lagrangian for a Light Dynamical "Higgs Particle"*, *Phys. Lett.* **B 722** (2013) 330 [*Erratum ibid.* **B 726** (2013) 926] [arXiv:1212.3305] [INSPIRE].

[15] G. Buchalla, O. Catà and C. Krause, *Complete Electroweak Chiral Lagrangian with a Light Higgs at NLO*, *Nucl. Phys.* **B 880** (2014) 552 [*Erratum ibid.* **B 913** (2016) 475] [arXiv:1307.5017] [INSPIRE].

[16] S.R. Coleman, J. Wess and B. Zumino, *Structure of phenomenological Lagrangians. 1.*, *Phys. Rev.* **177** (1969) 2239 [INSPIRE].

[17] C.G. Callan Jr., S.R. Coleman, J. Wess and B. Zumino, *Structure of phenomenological Lagrangians. 2.*, *Phys. Rev.* **177** (1969) 2247 [INSPIRE].

[18] T. Appelquist and C.W. Bernard, *Strongly Interacting Higgs Bosons*, *Phys. Rev.* **D 22** (1980) 200 [INSPIRE].

[19] A.C. Longhitano, *Heavy Higgs Bosons in the Weinberg-Salam Model*, *Phys. Rev.* **D 22** (1980) 1166 [INSPIRE].

[20] A.C. Longhitano, *Low-Energy Impact of a Heavy Higgs Boson Sector*, *Nucl. Phys.* **B 188** (1981) 118 [INSPIRE].

[21] F. Feruglio, *The Chiral approach to the electroweak interactions*, *Int. J. Mod. Phys.* **A 8** (1993) 4937 [hep-ph/9301281] [INSPIRE].

[22] M.E. Peskin and T. Takeuchi, *Estimation of oblique electroweak corrections*, *Phys. Rev.* **D 46** (1992) 381 [INSPIRE].

[23] A. Dobado, D. Espriu and M.J. Herrero, *Chiral Lagrangians as a tool to probe the symmetry breaking sector of the SM at LEP*, *Phys. Lett.* **B 255** (1991) 405 [INSPIRE].

[24] R.L. Delgado, A. Dobado, M.J. Herrero and J.J. Sanz-Cillero, *One-loop $\gamma\gamma \to W_L^+W_L^-$ and $\gamma\gamma \to Z_LZ_L$ from the Electroweak Chiral Lagrangian with a light Higgs-like scalar*, *JHEP* **07** (2014) 149 [arXiv:1404.2866] [INSPIRE].

[25] J.J. Sanz-Cillero, *Electroweak chiral Lagrangians and the Higgs properties at the one-loop level*, *EPJ Web Conf.* **80** (2014) 00053 [arXiv:1409.6517] [INSPIRE].

[26] I. Brivio, J. Gonzalez-Fraile, M.C. Gonzalez-Garcia and L. Merlo, *The complete HEFT Lagrangian after the LHC Run I*, *Eur. Phys. J.* **C 76** (2016) 416 [arXiv:1604.06801] [INSPIRE].

[27] A. Pich, I. Rosell and J.J. Sanz-Cillero, *Viability of strongly-coupled scenarios with a light Higgs-like boson*, *Phys. Rev. Lett.* **110** (2013) 181801 [arXiv:1212.6769] [INSPIRE].

[28] A. Pich, I. Rosell and J.J. Sanz-Cillero, *Oblique S and T Constraints on Electroweak Strongly-Coupled Models with a Light Higgs*, *JHEP* **01** (2014) 157 [arXiv:1310.3121] [INSPIRE].

[29] ATLAS collaboration, *Search for Heavy Resonances Decaying to a W or Z Boson and a Higgs Boson in the $q\bar{q}^{(\prime)}b\bar{b}$ Final State in pp Collisions at $\sqrt{s} = 13$ TeV with the ATLAS Detector*, ATLAS-CONF-2017-018 (2017).

JHEP03(2018)159

[30] CMS collaboration, *Search for heavy resonances that decay into a vector boson and a Higgs boson in hadronic final states at* $\sqrt{s} = 13$ *TeV*, *Eur. Phys. J.* **C 77** (2017) 636 [arXiv:1707.01303] [INSPIRE].

[31] H. Huang, *Searches for diboson resonances at CMS*, in *5th Large Hadron Collider Physics Conference (LHCP 2017)*, Shanghai China (2017) [arXiv:1710.05230] [INSPIRE].

[32] CMS collaboration, *Combination of searches for heavy resonances decaying to WW, WZ, ZZ, WH and ZH boson pairs in proton-proton collisions at* $\sqrt{s} = 8$ *and* 13 *TeV*, *Phys. Lett.* **B 774** (2017) 533 [arXiv:1705.09171] [INSPIRE].

[33] G. Buchalla, O. Catá and C. Krause, *On the Power Counting in Effective Field Theories*, *Phys. Lett.* **B 731** (2014) 80 [arXiv:1312.5624] [INSPIRE].

[34] A. Pich, I. Rosell, J. Santos and J.J. Sanz-Cillero, *Low-energy signals of strongly-coupled electroweak symmetry-breaking scenarios*, *Phys. Rev.* **D 93** (2016) 055041 [arXiv:1510.03114] [INSPIRE].

[35] A. Pich, I. Rosell, J. Santos and J.J. Sanz-Cillero, *Fingerprints of heavy scales in electroweak effective Lagrangians*, *JHEP* **04** (2017) 012 [arXiv:1609.06659] [INSPIRE].

[36] R.L. Delgado, A. Dobado and F.J. Llanes-Estrada, *Light 'Higgs', yet strong interactions*, *J. Phys.* **G 41** (2014) 025002 [arXiv:1308.1629] [INSPIRE].

[37] S. Dawson and G. Valencia, *Heavy fermion effects on longitudinal gauge boson scattering*, *Phys. Lett.* **B 246** (1990) 156 [INSPIRE].

[38] S. Weinberg, *Phenomenological Lagrangians*, *Physica* **A 96** (1979) 327 [INSPIRE].

[39] A. Manohar and H. Georgi, *Chiral Quarks and the Nonrelativistic Quark Model*, *Nucl. Phys.* **B 234** (1984) 189 [INSPIRE].

[40] R.L. Delgado, A. Dobado and F.J. Llanes-Estrada, *One-loop* $W_L W_L$ *and* $Z_L Z_L$ *scattering from the electroweak Chiral Lagrangian with a light Higgs-like scalar*, *JHEP* **02** (2014) 121 [arXiv:1311.5993] [INSPIRE].

[41] ATLAS and CMS collaborations, *Measurements of the Higgs boson production and decay rates and constraints on its couplings from a combined ATLAS and CMS analysis of the LHC pp collision data at* $\sqrt{s} = 7$ *and* 8 *TeV*, *JHEP* **08** (2016) 045 [arXiv:1606.02266] [INSPIRE].

[42] J.A. Aguilar-Saavedra, J. Bernabéu, V.A. Mitsou and A. Segarra, *The Z boson spin observables as messengers of new physics*, *Eur. Phys. J.* **C 77** (2017) 234 [arXiv:1701.03115] [INSPIRE].

[43] E. Maina, *W boson polarization in vector boson scattering at the LHC*, contribution to the *EPS-HEP international conference on high energy physics*, Venice Italy (2017), https://indico.cern.ch/event/466934/contributions/2575374/.

[44] R.L. Delgado, A. Dobado and F.J. Llanes-Estrada, *Unitarity, analyticity, dispersion relations and resonances in strongly interacting* $W_L W_L$, $Z_L Z_L$ *and* hh *scattering*, *Phys. Rev.* **D 91** (2015) 075017 [arXiv:1502.04841] [INSPIRE].

[45] R.L. Delgado, A. Dobado and F.J. Llanes-Estrada, *Possible new resonance from* $W_L W_L$*-*hh *interchannel coupling*, *Phys. Rev. Lett.* **114** (2015) 221803 [arXiv:1408.1193] [INSPIRE].

[46] A. Dobado, M.J. Herrero and T.N. Truong, *Unitarized Chiral Perturbation Theory for Elastic Pion-Pion Scattering*, *Phys. Lett.* **B 235** (1990) 134 [INSPIRE].

JHEP03(2018)159

[47] A. Dobado and J.R. Pelaez, *A Global fit of $\pi\pi$ and πK elastic scattering in ChPT with dispersion relations*, *Phys. Rev.* **D 47** (1993) 4883 [hep-ph/9301276] [INSPIRE].

[48] A. Dobado and J.R. Pelaez, *The Inverse amplitude method in chiral perturbation theory*, *Phys. Rev.* **D 56** (1997) 3057 [hep-ph/9604416] [INSPIRE].

[49] E. Halyo, *Technidilaton or Higgs?*, *Mod. Phys. Lett.* **A 8** (1993) 275 [INSPIRE].

[50] W.D. Goldberger, B. Grinstein and W. Skiba, *Distinguishing the Higgs boson from the dilaton at the Large Hadron Collider*, *Phys. Rev. Lett.* **100** (2008) 111802 [arXiv:0708.1463] [INSPIRE].

[51] P. Masjuan, J.J. Sanz-Cillero and J. Virto, *Some Remarks on the Pade Unitarization of Low-Energy Amplitudes*, *Phys. Lett.* **B 668** (2008) 14 [arXiv:0805.3291] [INSPIRE].

[52] T. Corbett, O.J.P. É boli and M.C. Gonzalez-Garcia, *Inverse amplitude method for the perturbative electroweak symmetry breaking sector: The singlet Higgs portal as a study case*, *Phys. Rev.* **D 93** (2016) 015005 [arXiv:1509.01585] [INSPIRE].

[53] A. Gomez Nicola and J.R. Pelaez, *Meson meson scattering within one loop chiral perturbation theory and its unitarization*, *Phys. Rev.* **D 65** (2002) 054009 [hep-ph/0109056] [INSPIRE].

[54] F.-K. Guo, P. Ruiz-Femenía and J.J. Sanz-Cillero, *One loop renormalization of the electroweak chiral Lagrangian with a light Higgs boson*, *Phys. Rev.* **D 92** (2015) 074005 [arXiv:1506.04204] [INSPIRE].

[55] T.N. Truong, *Chiral Perturbation Theory and Final State Theorem*, *Phys. Rev. Lett.* **61** (1988) 2526 [INSPIRE].

[56] A. Dobado, M.J. Herrero, J.R. Pelaez and E. Ruiz Morales, *CERN LHC sensitivity to the resonance spectrum of a minimal strongly interacting electroweak symmetry breaking sector*, *Phys. Rev.* **D 62** (2000) 055011 [hep-ph/9912224] [INSPIRE].

[57] D. Espriu and F. Mescia, *Unitarity and causality constraints in composite Higgs models*, *Phys. Rev.* **D 90** (2014) 015035 [arXiv:1403.7386] [INSPIRE].

[58] D. Espriu, F. Mescia and B. Yencho, *Radiative corrections to WL WL scattering in composite Higgs models*, *Phys. Rev.* **D 88** (2013) 055002 [arXiv:1307.2400] [INSPIRE].

[59] D. Espriu and B. Yencho, *Longitudinal WW scattering in light of the "Higgs boson" discovery*, *Phys. Rev.* **D 87** (2013) 055017 [arXiv:1212.4158] [INSPIRE].

[60] J.F. Owens, A. Accardi and W. Melnitchouk, *Global parton distributions with nuclear and finite-Q^2 corrections*, *Phys. Rev.* **D 87** (2013) 094012 [arXiv:1212.1702] [INSPIRE].

[61] ATLAS collaboration, *Search for high-mass diboson resonances with boson-tagged jets in proton-proton collisions at $\sqrt{s} = 8$ TeV with the ATLAS detector*, *JHEP* **12** (2015) 055 [arXiv:1506.00962] [INSPIRE].

[62] ATLAS collaboration, *Search for new resonances decaying to a W or Z boson and a Higgs boson in the $\ell^+\ell^- b\bar{b}$, $\ell\nu b\bar{b}$ and $\nu\bar{\nu}b\bar{b}$ channels with pp collisions at $\sqrt{s} = 13$ TeV with the ATLAS detector*, *Phys. Lett.* **B 765** (2017) 32 [arXiv:1607.05621] [INSPIRE].

JHEP03(2018)159